

# Characteristics of water-soluble polythiophene: TiO<sub>2</sub> composite and its application in photovoltaics

Qiquan Qiao

*Energy Conversion Systems Laboratory, Department of Mechanical Engineering, Virginia Commonwealth University, Richmond, Virginia 23284*

Lianyong Su

*Department of Chemistry, Virginia Commonwealth University, Richmond, Virginia 23284*

James Beck and James T. McLeskey, Jr.<sup>a)</sup>

*Energy Conversion Systems Laboratory, Department of Mechanical Engineering, Virginia Commonwealth University, Richmond, Virginia 23284*

(Received 10 June 2005; accepted 30 September 2005; published online 10 November 2005)

We have studied the characteristics of composites of an environmentally friendly water-soluble polythiophene sodium poly[2-(3-thienyl)-ethoxy-4-butylsulfonate] (PTEBS) and TiO<sub>2</sub>. We observed that the ultraviolet-visible absorption spectrum of low molecular weight PTEBS is redshifted possibly due to the formation of aggregates. Cyclic voltammetry reveals the values of highest occupied molecular orbitals and lowest unoccupied molecular orbitals for PTEBS. A factor of 7 in photoluminescence quenching indicates that the exciton dissociation and charge separation occur successfully at the PTEBS:TiO<sub>2</sub> (1:1 by weight) interface. This enhances the possibility that the separated charges will reach the electrodes before recombining. Scanning electron micrograph images show how the PTEBS and TiO<sub>2</sub> are interconnected and form paths to the electrodes to improve charge transport. Photovoltaic devices with TiO<sub>2</sub>:PTEBS composite achieved an energy conversion efficiency of  $\eta=0.015\%$ , a short circuit current of  $J_{SC}=0.22$  mA/cm<sup>2</sup>, an open circuit voltage of  $V_{OC}=0.72$  V, and a fill factor of FF=0.29 under  $\sim 300$  mW/cm<sup>2</sup> white light illumination. © 2005 American Institute of Physics. [DOI: 10.1063/1.2130517]

## I. INTRODUCTION

Composites of conjugated polymers and semiconductor nanocrystals or quantum dots are currently subject of intense investigation due to their wide application in electronic and optoelectronic devices. In the devices, the band structures and energy levels of the polymers and nanocrystals are chosen so that excitons dissociate at their interfaces. Photoexcited charge separation and recombination at these interfaces have attracted more attention and are being studied extensively.<sup>1,2</sup>

Most conjugated polymers have a band gap between the highest occupied molecular orbitals (HOMOs) and the lowest unoccupied molecular orbitals (LUMOs) in the range of 1.5–3 eV. This makes them well matched to the visible-light range and suitable for photovoltaic devices. The absorption spectra can be more finely tuned by modification of chemical structure of the polymers.<sup>3</sup> In addition, they are lightweight and flexible and are easy to use for device fabrication. However, these materials suffer from low charge mobility and short exciton diffusion lengths.<sup>4</sup> Furthermore, the photogenerated excitons are strongly bound. Therefore, the transfer and collection of charges are poor and photovoltaic devices made from homogeneous layers of these polymers have been inefficient.<sup>5</sup>

Due to their size and other properties, semiconductor nanocrystals or quantum dots offer a potential solution to

these deficiencies. The nanocrystals can be blended with the polymers to form heterojunctions.<sup>6,7</sup> It has been discovered that charge separation tends to occur at a material interface<sup>8</sup> because the excited electrons will transfer to the conduction band of the nanocrystals. The charge transfer is energetically favorable if the polymer and nanocrystals have different electron affinities.<sup>5</sup> Normally, the nanocrystals serve as the electron acceptor due to their higher electron affinity while the polymers act as electron donors.<sup>3</sup> Semiconductor nanocrystals or quantum dots including TiO<sub>2</sub>,<sup>4,9</sup> CdSe,<sup>3,5</sup> CdS,<sup>10</sup> carbon fullerenes,<sup>11,12</sup> and carbon nanotubes<sup>13–15</sup> have been reported for photovoltaic applications. The external energy conversion efficiencies of solar cells made from composites of conjugated polymers and semiconductor nanocrystals have increased steadily in the past decade.<sup>16</sup>

Solvent-based conjugated polymers such as poly(phenylene-vinylene)<sup>15</sup> (PPV) and its derivatives [MEH-PPV (Refs. 4 and 17) and MDMO-PPV (Refs. 18–20)] have been widely studied as photovoltaic materials.<sup>21</sup> Characteristics of hybrid composites made from the semiconductor nanocrystals and polymers such as poly(N-vinylcarbazole),<sup>22</sup> (PKV) and polyferrocenes<sup>1</sup> have also investigated. Polythiophenes are promising as materials in organic solar cells because they are chemically stable in ambient conditions and can form good contacts with metal electrodes.<sup>23</sup> Various groups have reported results using such polythiophene derivatives as poly(3-hexylthiophene)<sup>14,16,24,25</sup> (P3HT) and poly(3-octylthiophene)<sup>13,26–28</sup> (P3OT). Recently, a water-soluble

<sup>a)</sup>Electronic mail: jtmcleskey@vcu.edu

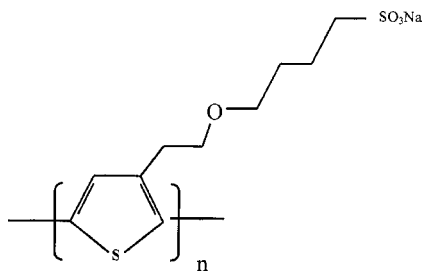


FIG. 1. Chemical structure of the water-soluble polythiophene (sodium poly[2-(3-thienyl)-ethoxy-4-butylsulfonate]).

thiophene polymer (sodium poly[2-(3-thienyl)-ethoxy-4-butylsulfonate]),<sup>29</sup> (PTEBS), has been investigated in organic photovoltaics.

## II. EXPERIMENT

In this paper, we study the characteristics of the blended PTEBS/TiO<sub>2</sub> composite and its application in photovoltaic devices. Transparent conductive fluorinated tin oxide (FTO) glass substrates with surface sheet resistance of 12.5–14.5 Ω/□ were purchased from Hartford Glass Co. Inc.<sup>30</sup> The substrates were cleaned in ultrasonic bath using acetone (10 min), 2-propanol (10 min), and de-ionized (DI) water (10 min). Colloidal TiO<sub>2</sub> powder (Degussa P25) was supplied by Degussa, USA.<sup>30</sup> The water-soluble polythiophene PTEBS was ordered from American Dye Source, Inc.<sup>31</sup> and its chemical structure is shown in Fig. 1.

The PTEBS was dissolved in DI water at a concentration of 15 mg/ml and a few drops of ammonium hydroxide were added for better dissolution. The solution was stirred for three days on a 40 °C heating plate to increase the solubility of PTEBS. The solution turns orange when PTEBS is satisfactorily dissolved. Two composite solution samples were then prepared by adding TiO<sub>2</sub> to the PTEBS solutions. The concentration of the TiO<sub>2</sub> relative to the PTEBS was 20 wt % (1 PTEBS:0.2 TiO<sub>2</sub>) and 100 wt % (1 PTEBS:1 TiO<sub>2</sub>). The solutions were sonicated for 4 h to disperse the TiO<sub>2</sub> powder and prevent the separated powder from aggregating again. A 300 μl solution of TiO<sub>2</sub>/PTEBS was drop cast on FTO substrates (2.5 × 2.5 cm<sup>2</sup>) until the whole surface was covered. Subsequently, the substrate with the solution on the surface was moved onto a 150 °C heating plate and dried. The drying temperature was kept below 260 °C to prevent the PTEBS from decomposing. Both the solution and film samples were prepared in air.

## III. RESULTS AND DISCUSSION

### A. UV-visible absorption spectrum

The absorption spectra of TiO<sub>2</sub>, PTEBS, and a PTEBS:TiO<sub>2</sub> composite (1:1 by weight) were measured with a Lambda 40 spectrometer and are shown in Fig. 2. The peak and line shape of the absorption in the composite indicate that it is the superposition of the absorption of PTEBS and TiO<sub>2</sub>. For wavelengths lower than 400 nm, the absorption of the composite has increased compared to the pure PTEBS and a new peak appears at 310 nm due to absorption by the TiO<sub>2</sub>. The line shape for wavelengths longer than 400 nm is

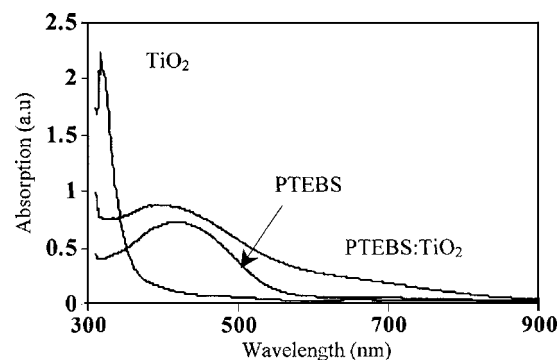


FIG. 2. Absorption spectra of PTEBS, TiO<sub>2</sub>, and 1:1 (by weight) PTEBS:TiO<sub>2</sub> composites on a FTO glass substrate.

similar to that of PTEBS, implying that absorption in this range is mainly due to the  $\pi$ - $\pi^*$  absorption of polymer. This means that no significant ground-state charge transfer or electronic interaction occurs between the two materials in the composite film under steady-state illumination at low intensities.<sup>32</sup> When illuminated in the white light, the photo-induced electrons are expected to transfer from the excited states of PTEBS to the conduction band of TiO<sub>2</sub>. This can be demonstrated by the quenching of the photoluminescence in the composite films and will be discussed in the next section.

Figure 2 reveals that with addition of TiO<sub>2</sub>, the absorption peak of PTEBS shifts to shorter wavelengths—a shift of 25 nm from 415 nm for pure PTEBS to 390 nm for PTEBS:TiO<sub>2</sub> composite. This can be explained in two ways. First, the absorption edge of TiO<sub>2</sub> around 400 nm increased the composite absorption and shifted the peak. The second may be that the TiO<sub>2</sub> prevents the formation of polymer aggregates in the composite films. van Hal *et al.*<sup>33</sup> reported that increasing the amount of TiO<sub>2</sub> from 1% to 50% to MDMO-PPV solutions caused the shifting of the absorption maximum to shorter wavelengths. Shi *et al.*<sup>34</sup> have also reported that polymers tend to form aggregates in solutions at high concentration. They observed that MEH-PPV solutions at concentrations of more than 1% lead to the development of strong aggregates in solid-state films. It is generally agreed that aggregates in polymer films lead to a redshift in both absorption and emission spectra.<sup>35</sup>

The pure PTEBS absorption spectrum shown in Fig. 2 is slightly different from that presented previously by Qiao and McLeskey.<sup>29</sup> As shown in Fig. 3, both the absorption maximum and its onset have shifted significantly to shorter wavelengths: from ~480 and 620 nm to 415 and 560 nm, respectively. The samples were purchased from American Dyes Source at separate times and the only difference is that the first sample has a low molecular weight (MW) while the second has a high molecular weight. In solution, the high MW PTEBS forms coils whereas the low MW PTEBS forms rodlike shapes. The absorption shift may occur because the interactions between the polymer chains in a rodlike conformation are stronger than between those in a coiled conformation.<sup>36</sup> As the polymer concentration is increased, the polymer chains come closer together and the interchain attraction forces become stronger. These interactions are maximized when the solutions are dried into solid-state

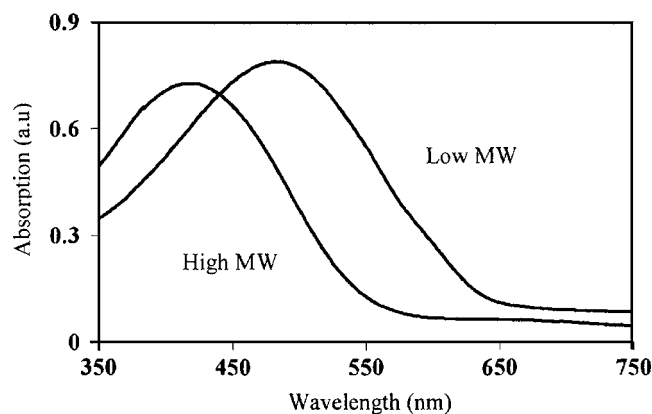


FIG. 3. The absorption spectra for drop cast film from low and high molecular weight PTEBS.

films.<sup>34</sup> Therefore, the more rodlike conformation solution leads to more aggregates in the films than that of coil conformation. As discussed above, the aggregates in the lower MW polymer films lead to a redshift in the absorption spectra. However, more future research needs to be done to verify why the significant change in the absorption occurs.

Figure 4 shows the electrochemical characterization of a cast film of PTEBS deposited on a FTO substrate. FTO glass was the working electrode. Platinum (Pt) and silver (Ag) were used as counter and quasireference electrodes, respectively. Potentials versus the Ag quasireference electrode were rescaled by saturated calomel electrode (SCE), calibrated with the ferrocene/ferrocenium redox couple (0.35 V vs Ag/AgCl,  $E_{SCE} = E_{Ag/AgCl} + 45$  mV). A computer-controlled potentiostat (Cypress System 1200) was used for electrochemical study. The electrochemical measurements were carried out with the scan rate of 200 mV/s in an electrolytic solution of CH<sub>3</sub>CN/LiClO<sub>4</sub> 0.1M in a glass cell. All the measurements were done at room temperature. As is shown in Fig. 4, the oxidation onset occurs at  $\sim +0.6$  V vs SCE. The HOMO level of PTEBS can be estimated at the onset point. Typically, an adjustment factor of 4.4–4.7 eV is used in converting the energy values versus SCE into energy values versus vacuum. Therefore, the HOMO level is estimated to be between  $-5.0$  and  $-5.3$  eV. The energy band gap of the high molecular weight of PTEBS from the absorption onset (560 nm), i.e., around 2.2 eV, which results in a LUMO level between  $-2.8$  and  $-3.1$  eV. Qiao and McLeskey<sup>29</sup> previously reported that HOMO of low MW PTEBS is approxi-

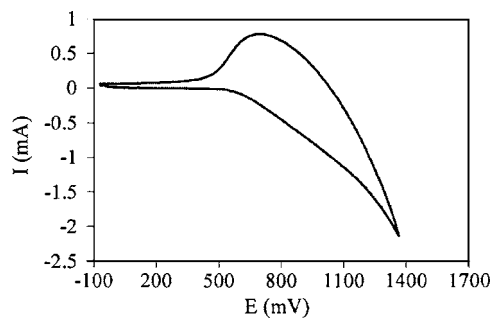


FIG. 4. Cyclic voltammogram (ref. SCE) of cast thin film of PTEBS on FTO substrate in CH<sub>3</sub>CN/LiClO<sub>4</sub> 0.1M.

mately  $-4.7$  to  $-5.1$  eV and its LUMO is about  $-2.7$  to  $-3.1$  eV, utilizing the results of cyclic voltamperometry measured by Tran-Van *et al.*<sup>37</sup>

## B. Photoluminescence spectra

Charge transfer is an important factor for good performance in solar cells and photoinduced charge transfer across the donor-acceptor junctions in composites offers a molecular approach to improving the solar cell efficiency.<sup>5,8,25,38–41</sup> Photoluminescence (PL) spectroscopy is one method for investigating the efficiency of the exciton dissociation and separation that occurs at the material interfaces in interdiffused polymer-nanocrystal composites. Because the diffusion range of singlet excitons of most conjugated polymers is approximately 5–15 nm and their radiative decays take place in the time of 100–1000 ps, a large area of nanosize interface in bulk heterojunction needs to be created so that the charge separation occurs faster than the radiative decay.<sup>3</sup> It has been shown<sup>10,16</sup> that the concentration of the nanocrystals affects the PL spectra and intensity. Photoluminescence occurs as a result of radiative decay. Its efficiency ( $\phi$ ) is determined by the fraction of absorbed photons ( $\eta$ ) that produce singlet excitons and the probability ( $\varepsilon$ ) that these singlets decay to the ground state via the radiative emission.<sup>32</sup> The expression is defined as

$$\phi = \eta \cdot \varepsilon.$$

Upon the incorporation of nanocrystals, either  $\eta$  or  $\varepsilon$  decreases due to the ultrafast electron transfer from the HOMO of polymer to the conduction band of the nanocrystals. This has been verified using a microwave conductivity technique.<sup>2</sup> Therefore, PL quenching occurring in the composite is caused by the existence and distribution of nanocrystals in the polymer matrix.

In addition, Salafsky<sup>32</sup> reported that the degree of the photoluminescent quenching is an indication of how well the nanocrystals are mixed in the polymer and the quality of polymer-nanocrystal interface. He presented a simple model explaining that the PL quenching caused by the dissociation of singlet excitons could be expressed as<sup>32</sup>

$$\Gamma = \eta \cdot \kappa,$$

where  $\Gamma$  is the possibility of charge separation events of an absorbed photon,  $\eta$  is the possibility of an absorbed photon resulting a state able to produce a singlet exciton, and  $\kappa$  is the efficiency of singlet exciton dissociation. Provided that the nonradiative decay caused by conformational defects in the polymer chains is negligible, all the absorbed photons take part in either PL or charge separation.

The PL intensity for the PTEBS/TiO<sub>2</sub> composites was measured using a 50 mW, 325 nm HeCd laser with a spot diameter of 4 mm. Figure 5 shows the PL of three different film samples. The first film was prepared from pure PTEBS, the second from a composite of 20% TiO<sub>2</sub> by weight of PTEBS, and the third from a composite of 100% TiO<sub>2</sub> by weight of PTEBS. All of the samples were on glass substrates coated with FTO. The laser was directly incident on the films and the PL was collected from the same side. To

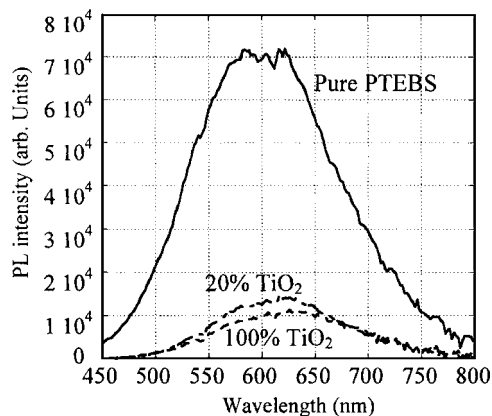


FIG. 5. The photoluminescence spectra from PTEBS:TiO<sub>2</sub> films for 0%, 20%, and 100% TiO<sub>2</sub>.

simplify the comparison, all the three films are approximately 10  $\mu\text{m}$  thick, which is thick enough to absorb nearly all of the light from the excitation laser.

As shown in Fig. 5, there is a significant quenching of the fluorescence in the composites as compared to the pure PTEBS. The PL is quenched by a factor of about 5 with the 20% TiO<sub>2</sub>. As the concentration of TiO<sub>2</sub> increases to 100%, the PL is further quenched to a factor of about 7. Although the polymer is a good hole conductor, the likelihood of recombination in pure polymer films is high because these materials suffer from low electron mobility and short exciton diffusion lengths.<sup>4</sup> In the polymer-TiO<sub>2</sub> bulk structures, PL quenching implies that the excitons dissociate and separate successfully at the interface of PTEBS (donor) and TiO<sub>2</sub> (acceptor). The polymer phase in the composites is continuous and forms favorable paths for holes throughout the film. However, charge transfer to the electrodes is still inhibited due to the limited paths for the separated electrons in the composite. This is because only some of the TiO<sub>2</sub> nanocrystals are in physical contact with each other,<sup>32</sup> leading to discontinuous paths for electrons. Recombination still occurs when the electrons leave the TiO<sub>2</sub> and reenter the polymer.<sup>10</sup> As more TiO<sub>2</sub> is added to the polymer, more of the TiO<sub>2</sub> nanocrystals are in physical contact with each other and the PL is quenched further as charge transfer improves.

### C. Scanning electron micrograph (SEM)

The morphology of the samples was studied using a LEO 440 *e*-beam writer. Scanning electron micrograph (SEM) images of a 1:0.2 composite of PTEBS:TiO<sub>2</sub> and a 1:1 composite of PTEBS:TiO<sub>2</sub> are shown in Fig. 6. In the 1:0.2 film [Fig. 6(a)], the TiO<sub>2</sub> nanocrystals agglomerated together and formed areas of densely packed TiO<sub>2</sub> bounded by regions of PTEBS. The size of the agglomerates ranges from a few hundred nanometers to micrometers.

Figure 6(b) shows the image from the 1:1 composite of PTEBS:TiO<sub>2</sub> at a magnification of 500 $\times$ . Two morphology structures have been demonstrated. From the amplified images at a magnification of 15 000 $\times$ , it can be seen that the structures in Figs. 6(c) and 6(d) are different. The explanation may be that, as compared to the 1:0.2 PTEBS:TiO<sub>2</sub>

composite, part of TiO<sub>2</sub> in the 1:1 composite fully agglomerated on the top and formed crystals as the solution was drop cast and dried on the heating plate.

As the percentage of TiO<sub>2</sub> increases, the size of the TiO<sub>2</sub> agglomerates increases and it is believed that more highly interpenetrated networks of TiO<sub>2</sub> are produced at higher concentrations. These networks form good paths for electrons and may help explain why the solar cells made using the 1:1 ratio of PTEBS to TiO<sub>2</sub> worked much better than the others. These results are consistent with those from CdSe and MEH-PPV composites made using transmission electron microscopy (TEM).<sup>10</sup>

### D. Application in organic solar cells

Polymer-based semiconductors have the potential to lower the cost of solar cells through the use of inexpensive liquid-based processing. A glass/FTO/TiO<sub>2</sub>:PTEBS/Au photovoltaic device structure was tested and is shown in Fig. 7. The active layer is composed of an interpenetrating network of nanocrystalline TiO<sub>2</sub> and PTEBS (a bulk heterojunction). The gold electrode was then sputter coated. The current-voltage (*I*-*V*) characteristics of the solar cells made from 1:1 PTEBS:TiO<sub>2</sub> composite were tested using a Keithley 236 source generator by sourcing the voltage from -2 to +2 V in 0.1 V steps both in the dark and under illumination. A solar simulator was used as the visible-light source to measure the efficiency. The devices were illuminated from the glass side due to the high transparency of the glass coated with FTO with the intensity of  $\sim 300$  mW/cm<sup>2</sup> measured using Spectra-Physics Model 407A power meter.

The current density-voltage (*J*-*V*) characteristics of the devices are shown in Fig. 8. The parameters of the photovoltaic devices such as short circuit current (*I*<sub>SC</sub>), open circuit voltage (*V*<sub>OC</sub>), fill factor (FF), and power conversion efficiency ( $\eta$ ) are all derived from Fig. 8. When no external voltage is applied to the solar cells, the built-in potential forces the photogenerated charges to drift and produce the short circuit current.<sup>42</sup> In addition, it is known that the short circuit current can be compensated to zero if a voltage equal to open circuit voltage is applied.<sup>42</sup> Therefore, the intersection of the *J*-*V* curve and the y axis is regarded as *I*<sub>SC</sub> and the meeting point of the curve and x axis is referred as *V*<sub>OC</sub>. *I*<sub>SC</sub> and *V*<sub>OC</sub> are the maximum current and voltage the devices can generate under the white light illumination, which can be measured using a multimeter. The fill factor represents a measure of the quality of the *J*-*V* characteristic and is defined as<sup>43</sup>

$$\text{FF} = \frac{(JV)_{\text{max}}}{I_{\text{SC}}V_{\text{OC}}}$$

where  $(JV)_{\text{max}}$  is highest power, which is the maximum product of *J* and *V* that can be calculated from the *J*-*V* curve. The energy conversion efficiency is defined as the ratio of the electric power output of the cell at the maximum power point to the incident optical power, which can also be expressed in terms of *I*<sub>SC</sub>, *V*<sub>OC</sub>, and FF as<sup>44</sup>

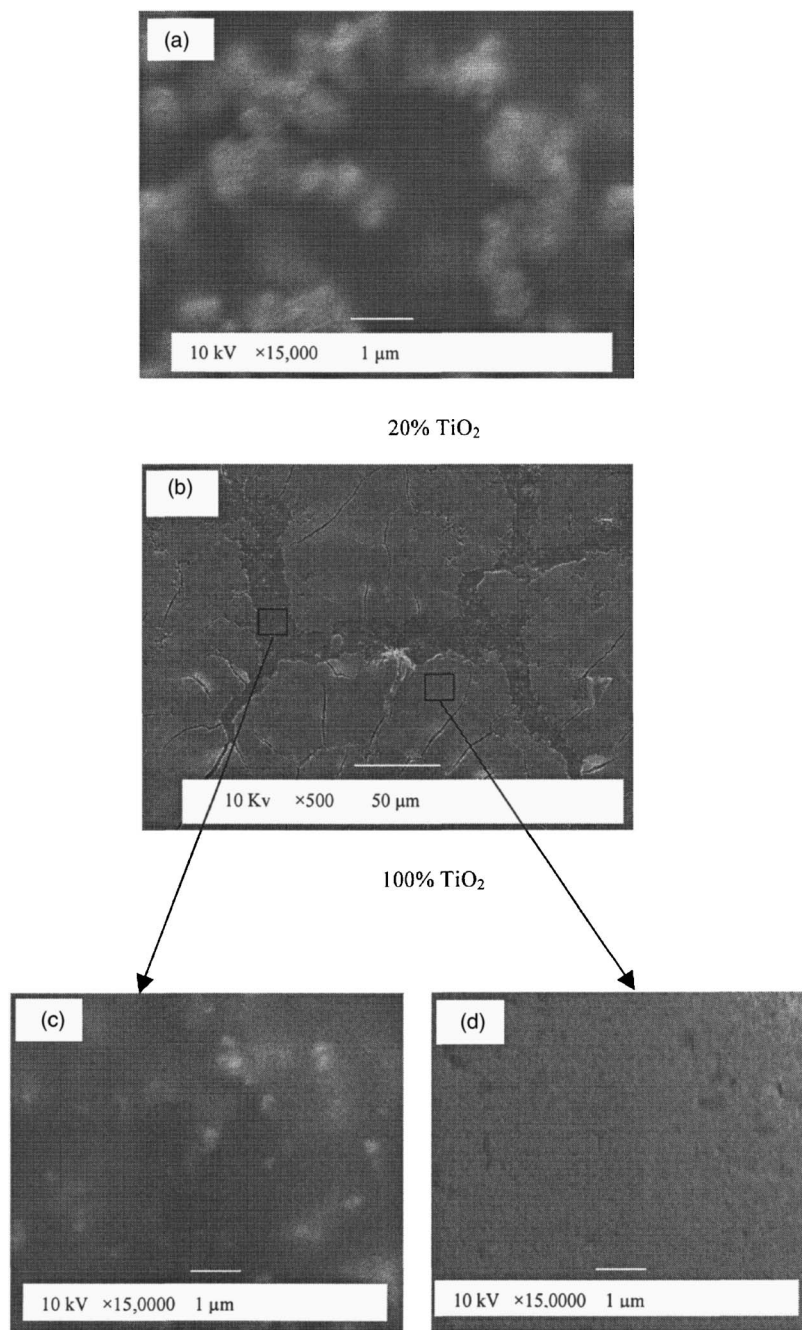


FIG. 6. SEM images of films from (a) PTEBS:TiO<sub>2</sub> (1:0.2), (b) PTEBS:TiO<sub>2</sub> (1:1), and [(c) and (d)] amplified SEM for PTEBS:TiO<sub>2</sub> (1:1).

$$\eta = \frac{FFV_{OC}J_{SC}}{P_{light}}$$

Based on the definitions above, the devices achieve an energy conversion efficiency of  $\eta=0.015\%$ , a short circuit current of  $J_{SC}=0.22 \text{ mA/cm}^2$ , an open circuit voltage of  $V_{OC}=0.72 \text{ V}$ , and a fill factor of  $FF=0.29$ . However, the solar cell performance is not stable. Of the cells that produced a notable voltage, it was interesting that the voltage slowly

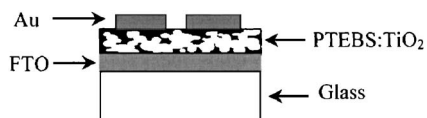


FIG. 7. Schematic of glass/FTO/TiO<sub>2</sub>:PTEBS/Au solar cells.

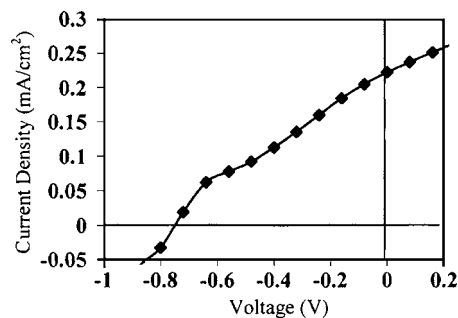


FIG. 8. The linear current density-voltage ( $J-V$ ) curve under the illumination of  $300 \text{ mW/cm}^2$ .

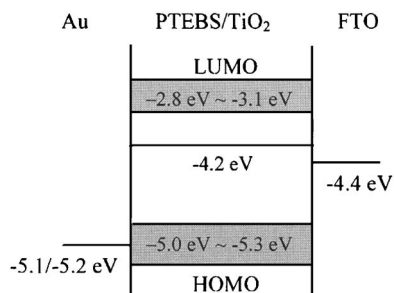


FIG. 9. Flatband energy diagram for the devices of FTO/TiO<sub>2</sub>:PTEBS/Au.

increased with time, as if electrons and holes were being slowly built up on the surface of the cell.

The performance of the devices depends, in part, on the carrier mobility. Typically, conjugated polymers such as PPVs and polythiophenes have electron mobilities of less than  $10^{-4}$  cm<sup>2</sup>/V s but hole transport mobilities of  $\sim 0.1$  cm<sup>2</sup>/V s.<sup>39</sup> To date, we have not measured the hole mobility of the PTEBS polymer film. However, based on the device performance, it is believed that the mobility of PTEBS polymer is similar to that of other polythiophenes. The TiO<sub>2</sub> acts as the electron acceptor and has an electron mobility of 0.1 cm<sup>2</sup>/V s.<sup>32</sup>

Based on the LUMO and HOMO obtained from the cyclic voltammogram, the flatband energy diagram for the devices of FTO/TiO<sub>2</sub>:PTEBS/Au is shown in Fig. 9. The open circuit voltage (0.72 V) can be estimated from the band diagram, which matches the difference between the gold (-5.1/5.2 eV) (Refs. 4 and 29) and the FTO (-4.4 eV) (Refs. 29 and 45) electrodes. Compared to the bilayer structure devices reported by Qiao and McLeskey,<sup>29</sup> the characteristics of the blended structure solar cells still need to be optimized. As found with the SEM, a layer of TiO<sub>2</sub> nanocrystals was formed on the top of the film, which may impede hole transport to the gold electrode. In future studies, the FTO (-4.4 eV) will be replaced with indium tin oxide (ITO) (4.7 eV) (Ref. 46) and the gold (5.1/5.2 eV) will be replaced by aluminum (4.3 eV).<sup>46</sup> By changing the relative work functions of the electrodes, it may be possible for the electrons to be transported through the TiO<sub>2</sub> to the aluminum and the holes be transported through the polymer chains to the ITO.

The emphasis of the reported work is on understanding the composite material properties rather than measuring device performance. However, previous work with PTEBS/TiO<sub>2</sub> in a bilayer configuration has led to devices with an efficiency of 0.13% under AM1.5 illumination.<sup>29</sup> Bulk heterojunction devices made with other materials have achieved power conversion efficiencies of P3HT/CdSe (1.7%),<sup>39</sup> P3HT/TiO<sub>2</sub> (0.424%),<sup>16</sup> P3OT/TiO<sub>2</sub> (0.06%),<sup>28</sup> etc. These differences can result from many factors including relative material properties (e.g., work functions), morphology, thickness, etc.

## IV. CONCLUSION

In summary, we have demonstrated that a composite of water-soluble PTEBS and TiO<sub>2</sub> has a potential in the appli-

cation of solar cells. UV-visible absorption spectra were measured and the optical band gap of PTEBS was determined to be approximately 2.2 eV. Charge transfer is preferential between high electron affinity TiO<sub>2</sub> (-4.2 eV) (Ref. 29) and relatively low ionization potential PTEBS (-2.8 to -3.1 eV). This was verified by the significant quenching of PL when the TiO<sub>2</sub> was mixed to form the high bulk interfacial area with the PTEBS. SEM has also revealed two different morphologies within the PTEBS:TiO<sub>2</sub> (1:1) film. The solar cells made using the composite showed promising photovoltaic results. In addition, because water is used as the solvent, the fabrication process is environmentally friendly. Future work needs to be done to improve the output and stability of the devices. The PTEBS polymer and the knowledge gained in this study may also be applicable to other organic electronic devices such as OLEDs and displays.

## ACKNOWLEDGMENTS

The authors are very grateful to Dr. Kenneth J. Wynne in Department of Chemical Engineering at Virginia Commonwealth University (VCU) and Dr. My T. Nguyen from American Dye Source, Inc. for the valuable discussions regarding the redshift in absorption spectra for the lower molecular weight PTEBS. The authors also would like to thank Dr. Hadis Morkoç, Dr. Ümit Özgür, and Yi Fu from Microelectronics Materials & Device Laboratory (MMDL) in Electrical and Computer Engineering at VCU for the assistance with the PL and the SEM. The authors also thank Dr. Fred M. Hawkrige of Chemistry Department in VCU for his help with the cyclic voltammogram.

<sup>1</sup>P. W. Cyr, M. Tzolov, M. A. Hines, I. Manners, E. H. Sargent, and G. D. Scholes, *J. Mater. Chem.* **13**, 2213 (2003).

<sup>2</sup>J. S. Salafsky, W. H. Lubberhuizen, and R. E. I. Schropp, *Chem. Phys. Lett.* **290**, 297 (1998).

<sup>3</sup>N. C. Greenham, X. Peng, and A. P. Alivisatos, *AIP Conf. Proc.* **404**, 295 (1997).

<sup>4</sup>A. C. Arango, S. A. Carter, and P. J. Brock, *Appl. Phys. Lett.* **74**, 1698 (1999).

<sup>5</sup>W. U. Huynh, X. Peng, and A. P. Alivisatos, *Adv. Mater. (Weinheim, Ger.)* **11**, 923 (1999).

<sup>6</sup>A. J. Nozik, *Physica E (Amsterdam)* **14**, 115 (2002).

<sup>7</sup>R. P. Raffaele, S. L. Castro, A. F. Hepp, and S. G. Bailey, *Prog. Photovoltaics* **10**, 433 (2002).

<sup>8</sup>G. Yu and A. J. Heeger, *J. Appl. Phys.* **78**, 4510 (1995).

<sup>9</sup>B. Oregan and M. Gratzel, *Nature (London)* **353**, 737 (1991).

<sup>10</sup>N. C. Greenham, X. Peng, and A. P. Alivisatos, *Phys. Rev. B* **54**, 17628 (1996).

<sup>11</sup>T. Piok, R. Schroeder, C. Brands, J. R. Hefflin, G. Leising, and W. Graupner, *Synth. Met.* **121**, 1589 (2001).

<sup>12</sup>G. Yu, J. Gao, J. C. Hummelen, F. Wudl, and A. J. Heeger, *Science* **270**, 1789 (1995).

<sup>13</sup>E. Kymakis and G. A. J. Amaratunga, *Sol. Energy Mater. Sol. Cells* **80**, 465 (2003).

<sup>14</sup>S. B. Lee, T. Katayama, H. Kajii, A. Araki, and K. Yoshino, *Synth. Met.* **121**, 1591 (2001).

<sup>15</sup>H. Ago, K. Petritsch, M. S. P. Shaffer, A. H. Windle, and R. H. Friend, *Adv. Mater. (Weinheim, Ger.)* **11**, 1281 (1999).

<sup>16</sup>C. Y. Kwong, W. C. H. Choy, A. B. Djurisic, P. C. Chui, K. W. Cheng, and W. K. Chan, *Nanotechnology* **15**, 1156 (2004).

<sup>17</sup>A. J. Breeze, Z. Schlesinger, and S. A. Carter, *Phys. Rev. B* **64**, 1 (2001).

<sup>18</sup>M. T. Rispens, A. Meetsma, R. Rittberger, C. J. Brabec, N. S. Sariciftci, and J. C. Hummelen, *Chem. Commun. (Cambridge)* **2003**, 2116.

<sup>19</sup>C. J. Brabec, S. E. Shaheen, T. Fromherz, F. Padinger, J. C. Hummelen, A. Dhanabalan, R. A. J. Janssen, and N. S. Sariciftci, *Synth. Met.* **121**, 1517 (2001).

- <sup>20</sup>C. J. Brabec, A. Cravino, D. Meissner, N. S. Sariciftci, M. T. Rispens, L. Sanchez, J. C. Hummelen, and T. Fromherz, *Thin Solid Films* **403–404**, 368 (2002).
- <sup>21</sup>H. Mattoussi, L. H. Radzilowski, B. O. Dabbousi, E. L. Thomas, M. G. Bawendi, and M. F. Rubner, *J. Appl. Phys.* **83**, 7965 (1998).
- <sup>22</sup>K. R. Choudhury, J. G. Winiarz, M. Samoc, and P. N. Prasad, *Appl. Phys. Lett.* **82**, 406 (2003).
- <sup>23</sup>R. Valaski, L. M. Moreira, L. Micaroni, and I. A. Hummelgen, *Braz. J. Phys.* **33**, 392 (2003).
- <sup>24</sup>C. Y. Kwong, A. B. Djuricic, P. C. Chui, K. W. Cheng, and W. K. Chan, *Chem. Phys. Lett.* **384**, 372 (2004).
- <sup>25</sup>W. U. Huynh, J. J. Dittmer, W. C. Libby, G. L. Whiting, and A. P. Alivisatos, *Adv. Funct. Mater.* **13**, 73 (2003).
- <sup>26</sup>E. Kymakis, I. Alexandrou, and G. A. J. Amaratunga, *J. Appl. Phys.* **93**, 1764 (2003).
- <sup>27</sup>E. Kymakis and G. A. J. Amaratunga, *Appl. Phys. Lett.* **80**, 112 (2002).
- <sup>28</sup>C. L. Huisman, A. Goossens, and J. Schoonman, *Synth. Met.* **138**, 237 (2003).
- <sup>29</sup>Q. Qiao and J. T. McLeskey, *Appl. Phys. Lett.* **86**, 153501 (2005).
- <sup>30</sup>G. Smestad, *Nanocrystalline Solar Cell Kit: Recreating Photosynthesis* (The Institute for Chemical Education, Madison, WI, 1998).
- <sup>31</sup>American Dye Source in <http://www.adsdyes.com/products/pdf/polythiophene/ADS2000P.pdf> 2002.
- <sup>32</sup>J. S. Salafsky, *Phys. Rev. B* **59**, 10885 (1999).
- <sup>33</sup>P. A. van Hal, M. M. Wienk, J. M. Kroon, W. J. H. Verhees, L. H. Slooff, W. J. H. van Gennip, P. Jonkheijm, and R. A. J. Janssen, *Adv. Mater. (Weinheim, Ger.)* **15**, 118 (2003).
- <sup>34</sup>Y. Shi, J. Liu, and Y. Yang, *J. Appl. Phys.* **87**, 4254 (2000).
- <sup>35</sup>J. W. Blatchford *et al.*, *Phys. Rev. B* **54**, 9180 (1996).
- <sup>36</sup>J. Ouyang, Q. Xu, C.-W. Chu, Y. Yang, G. Li, and J. Shinar, *Polymer* **45**, 8443 (2004).
- <sup>37</sup>F. Tran-Van, M. Carrier, and C. Chevrot, *Synth. Met.* **142**, 251 (2004).
- <sup>38</sup>N. S. Sariciftci, D. Braun, C. Zhang, V. I. Srdanov, A. J. Heeger, G. Stucky, and F. Wudl, *Appl. Phys. Lett.* **62**, 585 (1993).
- <sup>39</sup>W. U. Huynh, J. J. Dittmer, and A. P. Alivisatos, *Science* **295**, 2425 (2002).
- <sup>40</sup>W. U. Huynh, X. G. Peng, and A. P. Alivisatos, *Adv. Mater. (Weinheim, Ger.)* **11**, 923 (1999).
- <sup>41</sup>W. U. Huynh, J. J. Dittmer, N. Teclemariam, D. J. Milliron, A. P. Alivisatos, and K. W. J. Barnham, *Phys. Rev. B* **67**, 115326 (2003).
- <sup>42</sup>G. G. Malliaras, J. R. Salem, P. J. Brock, and J. C. Scott, *J. Appl. Phys.* **84**, 1583 (1998).
- <sup>43</sup>M. M. Alam and S. A. Jenekhe, *Chem. Mater.* **16**, 4647 (2004).
- <sup>44</sup>S. A. Jenekhe and S. J. Yi, *Appl. Phys. Lett.* **77**, 2635 (2000).
- <sup>45</sup>Q. Qiao, J. Beck, R. Lumpkin, J. Pretko, and J. T. McLeskey, Jr., *Sol. Energy Mater. Sol. Cells* **15**, July, 2005, <http://www.sciencedirect.com/science/journal/09270248>.
- <sup>46</sup>E. Arici, N. S. Sariciftci, and D. Meissner, *Adv. Funct. Mater.* **13**, 165 (2003).